A&A 421, L13–L16 (2004)
DOI: 10.1051/0004-6361:20040170

Astronomy & Astrophysics

Two new "very hot Jupiters" among the OGLE transiting candidates⋆

F. Bouchy[1,2], F. Pont[1], N. C. Santos[3,2], C. Melo[4], M. Mayor[2], D. Queloz[2], and S. Udry[2]

[1] Laboratoire d'Astrophysique de Marseille, Traverse du Siphon, BP 8, 13376 Marseille Cedex 12, France
[2] Observatoire de Genève, 51 Ch. des Maillettes, 1290 Sauverny, Switzerland
[3] Centro de Astronomia e Astrofísica da Universidade de Lisboa, Tapada da Ajuda, 1349-018 Lisboa, Portugal
[4] European Southern Observatory, Casilla 19001, Santiago 19, Chile

Received 14 April 2004 / Accepted 12 May 2004

Abstract. As a result of a radial velocity follow-up of OGLE planetary transit candidates in Carina, we report the discovery of two new transiting planets with very short orbital periods: OGLE-TR-113 with $m = 1.35 \pm 0.22\ M_{\rm Jup}$, $r = 1.08^{+0.07}_{-0.05}\ R_{\rm Jup}$, $P = 1.43$ days, and OGLE-TR-132 with $m = 1.01 \pm 0.31\ M_{\rm Jup}$, $r = 1.15^{+0.80}_{-0.13}\ R_{\rm Jup}$, $P = 1.69$ days. These detections bring to three the number of known "very hot Jupiter" (Jovian exoplanets like OGLE-TR-56 with periods around 1.5 days). This indicates that the accumulation of periods around 3 days found in radial velocity surveys does not reflect an absolute limit.

Key words. techniques: radial velocities – instrumentation: spectrographs – stars: planetary systems

1. Introduction

Since 1995, more than 120 planetary candidates have been discovered, mainly by radial velocity surveys. Although they provide a lot of information concerning the orbital parameters and the host star properties, such surveys do not yield the real mass of the planet (only $m \sin i$) and do not give any information about its size. The discovery of HD209458 by Doppler measurements (Mazeh et al. 2000) and photometric transit (Charbonneau et al. 2000; Henry et al. 2000) led to the first complete characterization of an extra-solar planet, illustrating the real complementarity of the two methods. The OGLE survey (Optical Gravitational Lensing Experiment) announced the detection of 137 short-period multi-transiting objects (Udalski et al. 2002a–c, 2003). Recently Konacki et al. (2003, 2004), thanks to a Doppler follow-up, announced the characterization of the first extra-solar planet with the unexpected extremely short period of 1.2 day, much below the lower end of the period distribution of planets detected by Doppler surveys (Udry et al. 2003). We present in this letter two new cases of extra-solar planets with very short orbital periods: OGLE-TR-113 and OGLE-TR-132.

2. Observations and reductions

The FLAMES facilities on the VLT (available since March 2003, Pasquini et al. 2002) is a very efficient way to conduct the Doppler follow-up of OGLE candidates. FLAMES is a multi-fiber link which feeds into the spectrograph UVES up to 7 targets on a field-of-view of 25 arcmin diameter in addition to the simultaneous thorium calibration. The fiber link produces a stable illumination at the entrance of the spectrograph and permits the use of simultaneous ThAr calibration in order to track instrumental drift. Forty-five minutes on a 17th magnitude star yield a signal-to-noise ratio (SNR) of about 8, corresponding to a photon noise uncertainty of about 30 $\rm m\,s^{-1}$ on a non-rotating K dwarf star. We have obtained 3.2 nights in visitor mode in March 2004 on this instrument (program 72.C-0191) in order to observe all OGLE candidates of the Carina field suspected to have a planetary companion (~20 candidates extracted from our re-analysis of photometric curves). We present here the results and the analysis of OGLE-TR-113 and OGLE-TR-132, two new cases of extra-solar planets with very short orbital periods. Results obtained on candidate OGLE-TR-131 are also presented to illustrate the precision of our radial velocity measurements. Results on all the other candidates will be included in Pont et al. (in preparation).

The spectra obtained from the FLAMES+UVES spectrograph were extracted using the standard ESO-pipeline with bias, flat-field and background correction. Wavelength calibration was performed with ThAr spectra. The radial velocities were obtained by weighted cross-correlation with a numerical mask constructed from the Sun spectrum atlas. The instrumental drift was computed by cross-correlation of the simultaneous ThAr spectrum with a thorium mask. Radial velocity errors were computed as a function of the SNR of the spectrum and the width (*FWHM*) of the Cross-Correlation Function (CCF)

Send offprint requests to: F. Bouchy,
e-mail: Francois.Bouchy@oamp.fr

⋆ Based on observations collected with the FLAMES+UVES spectrograph at the VLT/UT2 Kueyen telescope (Paranal Observatory, ESO, Chile: program 72.C-0191).

Table 1. Radial velocity measurements (in the barycentric frame) and CCF parameters for OGLE-TR-113, 131 and 132.

BJD [−2 453 000 d]	*RV* [km s^{-1}]	depth [%]	*FWHM* [km s^{-1}]	*SNR*	σ_{RV} [km s^{-1}]
OGLE-113					
78.60419	−7.862	40.23	9.4	11.0	0.041
79.64235	−8.268	40.07	9.5	11.7	0.040
80.65957	−7.931	39.73	9.6	10.2	0.042
81.59492	−7.858	38.94	9.5	9.3	0.043
82.71279	−8.077	40.19	9.5	11.5	0.041
83.66468	−8.098	39.60	9.4	10.8	0.041
84.65149	−7.574	40.91	9.4	12.0	0.040
85.60720	−8.027	40.32	9.4	11.5	0.041
OGLE-131					
78.57421	18.902	20.40	11.0	3.2	0.093
79.69280	18.944	36.18	10.5	7.5	0.049
80.69588	18.910	33.25	10.8	6.0	0.057
81.72914	19.001	32.90	10.2	5.8	0.056
82.64055	19.066	31.21	10.6	4.9	0.064
83.70039	18.954	33.55	10.1	6.2	0.054
84.61585	19.016	27.87	10.3	4.5	0.067
85.64254	18.879	28.34	10.6	4.6	0.067
OGLE-132					
81.72913	39.724	30.90	10.0	9.0	0.045
82.64054	39.700	29.41	10.3	7.6	0.049
83.70038	39.564	31.09	10.0	9.6	0.044
84.61585	39.822	30.56	10.3	8.2	0.047
85.64254	39.493	30.66	10.1	8.7	0.045

through the following relation based on photon noise simulations: $\sigma_{RV} = 0.025\, FWHM/SNR$.

However, our measurements are clearly not photon noise limited and we added quadratically an error of 35 m s^{-1} in order to take into the account systematic errors probably due to wavelength calibration errors, fiber-to-fiber contamination, and residual cosmic rays. This value is based on our experience with FLAMES+UVES and confirmed by the velocity residuals for OGLE-TR-131.

3. Results

3.1. Radial velocities

Our radial velocity measurements are listed in Table 1. Figure 1 shows the radial velocity data phased with the period and transit epoch from Udalski et al. (2002c, 2003). If the radial velocity variations are caused by the transiting objects, then phase $\phi = 0$ must correspond to the passage of the curve at center-of-mass velocity with decreasing velocity, which provides a further constraint. We fitted the data with a sinusoid (assuming a circular orbit) and determined the velocity semi-amplitude K and the center-of-mass velocity V_0. The orbital parameters are reported in Table 2.

The existence of an orbital signal for OGLE-TR-113 is clear. No significant Doppler variations are detected in OGLE-TR-131. The radial velocity residuals of 60 m s^{-1} are coherent with our estimation of uncertainties. For OGLE-TR-132, the reduced χ^2 of a constant velocity curve

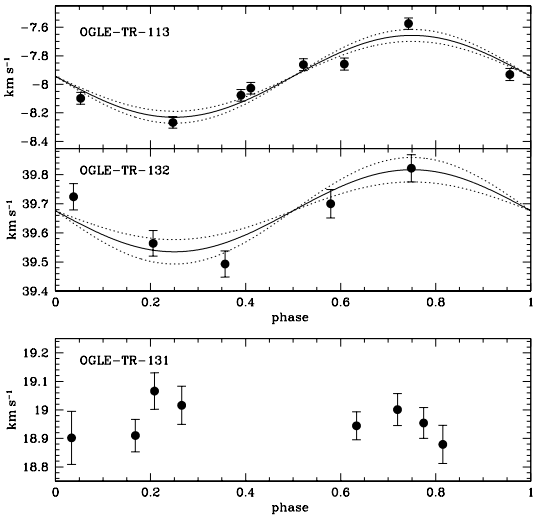

Fig. 1. Phase-folded Doppler measurements of OGLE-TR-113, 132 and 131. The dotted lines correspond to fit curves for lower and upper 1-sigma intervals in semi-amplitude K.

without orbital motion is 33.1 ($P(\chi^2) \sim 10^{-6}$). Even if unrecognized systematics caused our error bars to be underestimated by a factor 1.5, the reduced χ^2 would still be 14.7 ($P(\chi^2) = 0.5\%$). As a foolproof check of the detection confidence, we also applied a bootstrap procedure to the data. Bootstrapping gives an estimation of the significance of a signal without any assumption on the size of the uncertainties (see e.g. Press et al. 1992). This yields a significant value of K ($K > 42$ m s^{-1}) in 97% of the cases. Therefore, even with the assumption of large unrecognized systematics, the detection of orbital motion for OGLE-TR-132 on the correct period and phase is robust (∼3 sigma detection).

We estimated from the CCFs the projected rotation velocity $v \sin i$ assuming a Gaussian instrumental profile *FWHM* of 9.2 km s^{-1}. For the three candidates, the $v \sin i$ is lower than 5 km s^{-1}, indicating that the primaries are not tidally locked with their companion and that the expected Rossiter effect is lower than our Doppler precision.

3.2. Spectral line bisectors and blend scenarios

It is known that in certain circumstances, the combination of a single star with a background unresolved eclipsing binary can mimic both a planet transit signal and velocity variations (Santos et al. 2002). If the velocity variations are caused by a background binary system, however, the CCF bisector is expected to vary. In order to examine the possibility that the radial velocity variation is due to a blend scenario, we computed the CCF bisectors as described by Santos et al. (2002). Figure 2 indicates that there is no correlation of the line asymmetries with phase and that the dispersion is well below the velocity signal amplitude. Furthermore the CCF was computed with different masks without significant change in the radial velocity values (as discussed by Santos et al. 2002, most blend scenarios produce mask-dependent velocities). Moreover, a background binary of such short period would be expected to be synchronized, and thus to show a cross-correlation function very

Table 2. Orbital and stellar spectroscopic parameters.

Name	$P_{\rm OGLE}$ [days]	$T0_{\rm OGLE}$ −2 452 000 d	K [km s^{-1}]	V_0 [km s^{-1}]	O−C [m s^{-1}]	$T_{\rm eff}$	$\log g$	[Fe/H]
OGLE-TR-113	1.43250	324.36394	0.287 ± 0.042	−7.944 ± 0.027	66	4752 ± 130 K	4.50 ± 0.53	0.14 ± 0.14
OGLE-TR-132	1.68965	324.70067	0.141 ± 0.042	39.676 ± 0.032	53	6411 ± 179 K	4.86 ± 0.14[a]	0.43 ± 0.18

[a] The unrealistically small value $\sigma_{\log g} = 0.14$ for 132 was replaced with $\sigma_{\log g} = 0.5$.

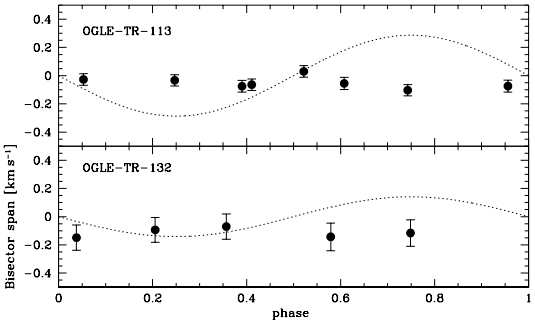

Fig. 2. Bisector span [$V_{\rm top} - V_{\rm bottom}$] of the three targets. Errors correspond to twice the radial velocity errors. Dotted lines correspond to the velocity signal from Fig. 1.

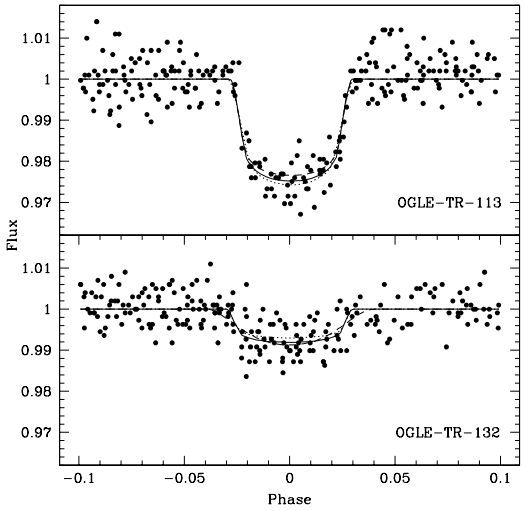

Fig. 3. Phase-folded normalized light curve and best-fit transit curve (solid line) for OGLE-TR-113 and OGLE-TR-132. The dotted and dashed lines correspond to fit curves for lower and upper 1-sigma intervals in r/R.

broadened by rotation. Simulations show that a broad background CCF contaminating a narrow foreground CCF is very inefficient in causing an apparent velocity variation. In order to provoke variations of the observed amplitude, any broadened background CCF would have to be large enough to be clearly visible in the total CCF, which is not the case. Therefore, the scenario "foreground single star plus background short-period eclipsing binary" can be eliminated with confidence. While other more intricate scenarios could conceivably be possible, we were not able to contrive any that could explain both the photometric and the velocity signals while remaining credible.

3.3. Spectral classification

On the summed spectra, the intensity and equivalent width of some spectral lines were analyzed to give temperature, gravity and metallicity estimates for the primaries in the manner described in Santos et al. (2004). The results are given in Table 2.

3.4. Light curve analysis and physical parameters

The shape of the transit light curve depends in a non-linear way on the latitude of the transit, the radius ratio r/R, and the factor $R(m+M)^{-1/3}$, where R, M, r, m are the radius and mass values for the primary and eclipsing planet respectively. Synthetic transit curves computed with the procedure of Mandel & Agol (2002) were fitted to the photometry data by least-squares (Fig. 3). A quadratic limb darkening with $u1 + u2 = 0.6$ was assumed (based on typical values in red filters from Barban et al. 2003). Some possible sources of systematic uncertainties are not taken into account in this letter: variations in the limb darkening coefficients, possible contamination by background stars, uncertainties in the stellar evolution predictions, uncertainties in the orbital period. They will be included in the paper presenting the complete spectroscopic follow-up (Pont et al., in preparation).

The values of the mass and radius of the primary, M and R, were obtained by combining the constraints from the transit shape (dependence on $RM^{-1/3}$) and from the spectroscopic determination of $T_{\rm eff}$, $\log g$ and [Fe/H] by χ^2 minimization, taking the relation between M, R, $T_{\rm eff}$, $\log g$ and [Fe/H] from an interpolation of Girardi et al. (2002) stellar evolution models. The value of r was then derived from r/R and R, and m from M and the semi-amplitude of the radial velocity orbit, assuming circular Keplerian motion with $\sin i = 1$. (The shortness of the period ensures that the orbits are circularized by tidal effects, and the presence of a transit indicates that $\sin i$ is very near to unity.) Table 3 summarizes the resulting physical parameters of OGLE-TR-113 and OGLE-TR132 and their planetary companions.

4. Discussion and conclusion

The parameters of OGLE-TR-113b are very accurately defined, first because the transit shape is clearly delineated by the photometric data, second because there is only a narrow range of possible parameters allowed by stellar evolution models for a cool K dwarf. As a result, r could be computed with a very small formal uncertainty (neglecting possible systematic errors as discussed above).

The photometric transit signal of OGLE-TR-132 is near the detectability limit, but the existence of a radial velocity

Table 3. Summary table with the physical parameters M, R, m, r, inclination angle i, semi-major axis a and average density ρ. The uncertainties do not take possible systematic errors into account.

Name	M $[M_\odot]$	R $[R_\odot]$	m $[M_{\rm Jup}]$	r $[R_{\rm Jup}]$	i [deg]	a [AU]	ρ [g cm^{-3}]
OGLE-113	0.77 ± 0.06	0.765 ± 0.025	1.35 ± 0.22	$1.08^{+0.07}_{-0.05}$	85−90	0.0228 ± 0.0006	1.3 ± 0.3
OGLE-132	1.34 ± 0.10	$1.41^{+0.49}_{-0.10}$	1.01 ± 0.31	$1.15^{+0.80}_{-0.13}$	78−90	0.0306 ± 0.0008	$0.8^{+0.4}_{-0.7}$

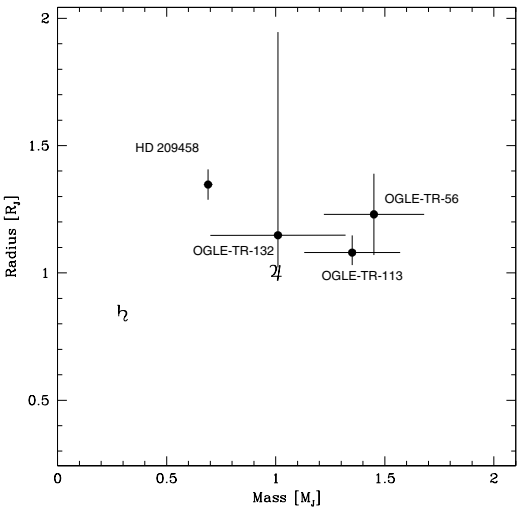

Fig. 4. The four known transiting extrasolar planets plotted in the Mass-Radius diagram. The symbols indicate Jupiter and Saturn.

variation at the precise period and phase of the transit gives confidence in the reality of the transiting companion. In contrast with OGLE-TR-113, the parameters are not very well constrained. The transit shape is too poorly defined to constrain the impact parameter, so that there is a strong degeneracy between the impact parameter and the primary radius R. Furthermore the values of temperature and gravity measured from the spectra are compatible with a wide variety of young to evolved F dwarfs, with radii ranging from 1.3 to 1.9 $R_\odot$. As a result, the upper uncertainty interval on r is wide. The light curve is compatible with either a central transit in front of a $R \sim 1.3\ R_\odot$ star, or a high-latitude transit in front of a $R \sim 1.9\ R_\odot$ star.

The detection of OGLE-TR-113b and OGLE-TR-132b show that the case of OGLE-TR-56 is not isolated and that "very hot Jupiters" (i.e. Jovian exoplanets with periods much smaller than 3 days) are not extremely uncommon. Therefore, the accumulation of hot Jupiters near periods of 3 days (Udry et al. 2003) does not reflect an absolute limit for the existence of planets. The parent stars of OGLE-TR-56, 113 and 132 are very different, ranging from F to K dwarfs, indicating that "very hot Jupiters" are possible around different types of stars.

Figure 4 gives the mass-radius relation for the four known transiting exoplanets. It is noteworthy that if OGLE-TR-132 is a low-latitude transit, then the three "very hot Jupiters" have a density markedly higher than HD209458b.

The two new detections bring to 3 the number of "very hot Jupiters" detected in the OGLE transit survey, among 155 000 light curves examined for transits. Given the geometric probability of transit (∼17% for $P = 1.5$ days), this result implies a total number of 21 ± 10 "very hot Jupiters" among the targets (binomial distribution), therefore one in every 5000 to 14 000 targets. The detection completeness of the OGLE survey toward transiting "very hot Jupiters" should be computed with detailed simulations, but it may be quite high because for such short period the phase coverage is very good. Even if there is a proportion of giants stars among the OGLE candidates that would have been weeded out of the radial velocity surveys, the absence of "very hot Jupiters" among the ∼3000 field dwarfs surveyed in radial velocity in the solar neighborhood is therefore not incompatible with our result. This estimate also indicates that "very hot Jupiters" are not out of reach of future radial velocity surveys. It is noteworthy though that for such low periods, photometric transit surveys are a more efficient detection method than radial velocity monitoring. We also note that the lack of hot Jupiters (with periods in the range 3−10 days) among the OGLE transiting candidates seems to be inconsistent with the frequency of ∼1% for hot Jupiters deduced from radial velocity surveys.

Acknowledgements. We are grateful to C. Moutou for very useful comments and J. Smoker for support at Paranal. F.P. gratefully acknowledges the support of CNRS through the fellowship program of CNRS. Support from Fundação para a Ciência e Tecnologia (Portugal) to N.C.S. in the form of a scholarship is gratefully acknowledged.

References

Barban, C., Goupil, M. J., Van't Veer-Menneret, C., et al. 2003, A&A, 405, 1095
Charbonneau, D., Brown, T. M., Latham, D., & Mayor, M. 2000, ApJ, 529, L45
Girardi, M., Manzato, P., Mezzetti, M., et al. 2002, ApJ, 569, 720
Henry, G., Marcy, G., Butler, R., & Vogt, S. 2000, ApJ, 529, L41
Konacki, M., Torres, G., Jha, S., et al. 2003a, Nature, 421, 507
Konacki, M., Torres, G., Sasselov, D., et al. 2004, ApJ, in press
Mandel, K., & Agol, E. 2002, ApJ, 580, 171
Mazeh, T., Naef, D., Torres, G., et al. 2000, ApJ, 532, L55
Pasquini, F., Avila, G., Blecha, A., et al. 2002, The Messenger, 110, 1
Pont, F., & Eyer, L. 2004, MNRAS, in press [arXiv:astro-ph/0401418]
Press, W. H., Teukolsky, S. A., Vetterling, W. T., & Flannery, B. P. 1992, Numerical recipes (Cambridge University Press), 690
Santos, N. C., Mayor, M., Naef, D., et al. 2002, A&A, 392, 215
Santos, N. C., Israelian, G., & Mayor, M. 2004, A&A, 415, 1153
Sirko, E., & Paczynski, B. 2003, ApJ, 592, 1217
Udalski, A., Paczynski, B., Zebrun, K., et al. 2002a, Acta Astron., 52, 1
Udalski, A., Zebrun, K., Szymarski, M., et al. 2002b, Acta Astron., 52, 115
Udalski, A., Zebrun, K., et al. 2002c, Acta Astron., 52, 317
Udalski, A., Pietrzynski, G., Szymarski, M., et al. 2003, Acta Astron., 53, 133
Udry, S., Mayor, M., & Santos, N. C. 2003, A&A, 407, 369